Al-Khwarizmi Engineering Journal, Vol. 5, No. 1, PP 20-32 (2009)

Al-Khwarizmi Engineering Journal

Mass Transfer Coefficient During Cathodic Protection of Low Carbon Steel in Seawater

Khalid W. Hameed *, **Anees Abdullah Khadom** ** and **Ameel Mohammed Rahman** *

**Department of Biochemical Engineering/ Al-Khwarizmi College of Engineering/University of Baghdad*

*** College of Engineering/ University of Daiyla*

(Received 19 June 2008; accepted 13 January 2009)

Abstract

The aim of this research is to calculate mass transfer coefficient, k_d, during cathodic protection of low carbon steel in neutral seawater (3.5% W/V *NaCl* in distilled water with pH = 7). Two types of cathodic protection were used:

First: Sacrificial anode cathodic protection (SACP) were a pipeline of steel carrying seawater using zinc as a sacrificial anode and with variable temperatures ranged (0 – 45^{o}C) and volumetric flow rate ranged (5 – 900 lit/hr). It was found that the k_d increases with increasing temperature and volumetric flow rate of seawater, where k_d ranged (0.24×10^{-6} – 41.6×10^{-6} m/s).

Second: Impressed current cathodic protection (ICCP) technique adopting a rotating vertical steel cylinder in seawater with variable temperatures ranged (0 – 45^{o}C) and rotating velocity ranged (0 – 400 rpm). It was found that the k_d increases with increasing temperature and rotating velocity, where k_d ranged (7.25×10^{-6} – 36.82×10^{-6} m/s).

Keywords: Cathodic Protection, Momentum Transfer, Reynolds Number, Carbon Steel

1. Introduction

Corrosion is an electrochemical process in which a current leaves a structure at the anode site, passes through an electrolyte and reenters the structure at the cathode site. Current flows because of a potential difference between the anode and cathode that is the anode potential is more negative than the cathode potential, and the difference is the driving force for the corrosion current. The total system-anode, cathode, electrolyte and metallic connection between anode and cathode is termed a corrosion cell [Shrier(1), 1976 and George, 1985].

Cathodic protection involves the application of a direct current (DC) from an anode through the electrolyte to the surface to be protected. This is often through of as "overcoming" the corrosion currents that exist on the structure. There is no flow of electrical currents (electrons) through the electrolyte but flow of ionic current. Cathodic protection eliminates the potential differences between the anodes and cathodes on the corroding surface. There are two proved methods of applying cathodic protection: sacrificial anode (galvanic) and impressed current. Each method depends upon a number of economic and technical considerations and as certain advantages. For every structure, there is a special cathodic protection system dependent on the environment of the structure [Scully, 1975].

When an electrode is polarized, the surface concentration of species that is either being oxidized or reduced fall to zero. Additional material will then diffuse to the electrode surface towards this region of lower concentration. If the electrolysis experiment is carried out in an agitated solution, i.e. the solution is in motion with respect to the electrode or vise versa, then the resulting concentration-distance profile at the electrode surface can be represented as shown in figure (1) [Trethewey and Chamberlain, 1996 and Roberge, 2004].

In the figure (1) the electrode is represented by bold bar in the left side of figure. The x-axis is a scalar and represents distance away from the electrode. They-axis represents concentration. The maximum concentration is represented by C_b

which is its concentration in the bulk solution. In figure (1) there are two regions of concentration. Because the solution is well mixed, in the bulk region the concentration is constant with respect to distance. This is represented by horizontal line where C = C_b (this is known as the convective region). There is then a region where the concentration drops, falling to zero at the electrode surface. The diffusion layer associated with this drop has thickness δ_d. the exact thickness of the diffusion layer depends upon the nature of the solution into which it extends. For stirred aqueous solution the thickness of the diffusion layer can between 0.001 to 0.01 mm Roberge, 2004].

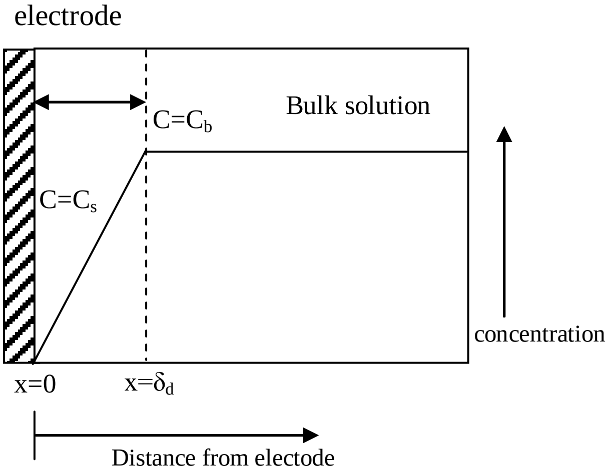

Fig.1. Variation of an Anion Concentration with Distance from Electrode [Roberge, 2004].

For an unstirred solution it is about 0.5 mm thick [Uhlig, 1971]. In an important assumption of this mode is that when material reaches the surface of the electrode it is instantaneously oxidized or reduced thereby maintaining a zero concentration at the electrode surface. In practice, this is easy to achieve by selecting a suitable polarization voltage.

It is clear that the concentration gradient in the diffusion layer, we not that it both linear and constant. It is can be represented gradient mathematically as:

$$\frac{dC}{dx}=\frac{(C_b-C_s)}{\delta_d} \quad ….(1)$$

Fick's law of diffusion state that [Shreir (1), 1976, and Trethewey, 1996]:

$$J=-D\frac{dC}{dx} \quad …(2)$$

Where J is the flux of substance and D is a diffusion coefficient. It can be seen from Faraday's law of electrolyte that:

$$i=zFJ \quad …(3)$$

Where i is the current density, $\mu A/cm^2$, z is the valancy number of electrons involved in reaction, eq/mol, and F is Farady's constant (96496), c/mol. From equations 1, 2, and 3:

$$i=-zFD\frac{(C_b-C_s)}{\delta_d} \quad …(4)$$

The negative sign is conventional, it us the current is being carried away from the cathode (as hydroxyl ion). The magnitude of current is interesting only and since, C_s can never be negative, and the magnitude of the current is great when C_s = 0, again the maximum or limiting current density:

$$i=-zFD\frac{C_b}{\delta_d} \quad …(5)$$

Notice that when $C_s > C_b$, the implication is that the concentration of species in the region of electrode is increasing. The resulting sign from negative to positive tell us the current is reversed [Trethewey and Chamberlain, 1996, Hanson, 2000 and Cottis, 2002].

The present work considered two types of cathodic protection. In the sacrificial anode cathodic protection , the effect of temperature (0 – 45°C) and flow rate (5 – 900 lit/h) on the mass transfer coefficient, k_d , are studied with constant pH = 7, duration time = 3 hrs and NaCl in distilled water = 3.5% W/V. In the impressed current cathodic protection, the effect studied were temperature (0 – 45°C), rotating velocity (0 – 400 rpm) on the k_d with constant pH = 7 and NaCl in distilled water = 3.5% W/V.

2. Experimental Work

I. Sacrificial Anode Cathodic Protection System:

Working electrode (cathode): working electrode was tube specimen of low carbon steel with dimensions of 13.50 cm length, 2.68 cm inside diameter and 0.23 cm thick. Anode electrode: Anode electrode was zinc strip with dimensions of 12.50 cm length, 1.00 cm width and 0.6 cm thick.

The chemical composition of tube specimen of low carbon steel and zinc strip were analyzed by Specialized Institute of Engineering Industries were as shown in table (1) and (2) respectively.

The apparatus shown in figure (2) [Champion,1964] was used to study the variables, temperature (0 – 45^{o}C) and flow rate (5 – 900 lit/h] on corrosion rate or zinc consumption rate to compare with the mass transfer coefficient k_d . After the container vessel was filled with seawater (3.5 % W/V NaCl solution) adjusting pH to 7 and temperature to the desired values. The zinc strip was weighted and fixed at the inlet of the steel tube by rubber stopper and was electrically connected by an insulated copper wire to the steel tube outlet as shown figure (2). The zinc strip is extended along the steel tube to ensure uniform current and potential distribution along the tube wall.

The seawater was pumped from the vessel by the pump through the rotameter to measure the desired flow rate, then the seawater inter from from the below the steel tube and out from upper the tube to return to the vessel again (i.e. the seawater is circulated between the vessel and steel tube). After each run the zinc strip was rinsed in distilled water and brush to remove the corrosion products, dried with clean tissue then immersed in the benzene and acetone, dried again and re-weighted to determine the weight loss and prepare for another experiment. The steel tube is also rinsed and dried by the same way above in order to re-use another time. After each run the vessel is emptied from the solution and washed with distilled water, then filled wit a new prepared solution for a new run.

Table 1,
Chemical Composition of Low Carbon Steel

C, %	0.1648
Si, %	0.2540
Mn, %	0.5101
S, %	0.0062
Cr, %	0.0253
Ni, %	0.0090
Cu, %	0.1511
V, %	0.0034
Fe, %	Rem.

Table 2,
Chemical Composition of Zinc Strip

Al, %	0.12
Pb, %	0.0034
Cu, %	0.0017
Cd, %	0.0033
Fe, %	0.0032
Sn, %	0.0023
Zn, %	Rem.

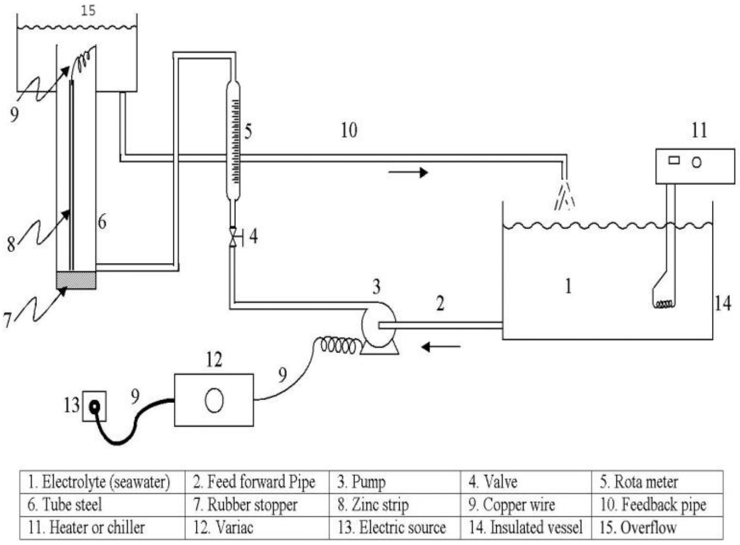

Fig.2. Schematic Diagram of Apparatus Used in Sacrificial Anode Test System.

II. Impressed Current System:

Working electrode (cathode): working electrode was cylinder specimen of low carbon steel with dimensions of 1.58 cm length, 2.33 cm outside diameter and 0.18 cm thick. The composition of steel is the same of that of low carbon steel which was illustrated in table (1).

Auxiliary: electrode (anode): auxiliary electrode was a rod of high conductivity graphite, 4.5 cm length and 0.8 cm outside diameter.

Reference electrode: the cathode potential is determined with respect to saturated calomel electrode (SCE).

A luggin capillary bridge leading to the reference electrode is mounted near the center of cathode to within one millimeter from the side of the cathode. The opening of the capillary tube near the cathode is equal to one millimeter in diameter

The apparatus shown in figure (3) was used in the polarization technique. [Cornet and Kappsser, 1969 and Harvey and Robert, 1988]. After preparing the seawater (3.5% W/V NaCl solution), and construct the electrochemical cell with desired variable of temperature and velocity, the circuit is switched on and the voltage of power supply is stabilized on 3.0 V. Changing the current by altering the resistance of the circuit, where at each setting of the resistance, two parameters are recorded (potential and cathodic current) by voltmeter and ammeter respectively. i.e. to measure the cathodic portion of the polarization curve. Two minutes at least were are allowed in order to record the steady state values of the polarization process. After reaching E_{corr} (steady state corrosion potential) of the steel specimen used, the run was ended by switched off the circuit and electrochemical cell is emptied from used seawater. The system is then washed with distilled water to ensure that there is no electrolyte left in the system. the above procedure is repeated exactly for other conditions of temperature and velocity. Each test was made twice and if reproducibility was in doubt a third was carried out.

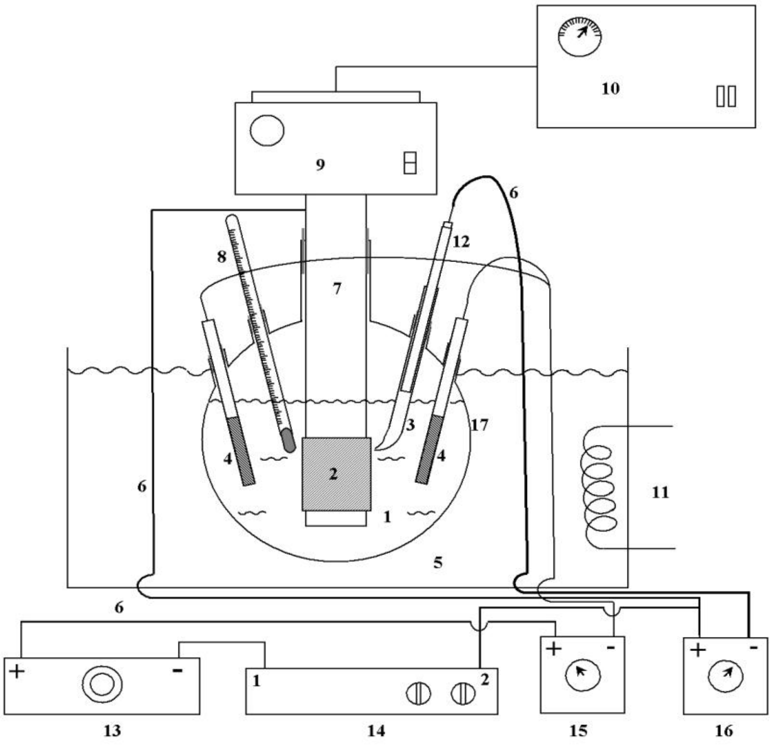

1- Electrolyte (Seawater)	2- Cylinder Steel Specimen	3- Luggin	4- Auxiliary anode (Graphite)	5- Water bath
6- Wires	7- Shaft motor	8- Thermometer	9- Motor	10- Speed control
11- Heating or cooling coil	12- SCE	13. power supply	14- Box Resistance	15- A meter
16- Voltmeter				

Fig.3. Schematic Diagram of Apparatus Used in Impressed Current Test System.

3. Results and Discussion

I. Sacrificial Anode Cathodic Protection System:

Zinc consumption rate: Before calculation of mass transfer coefficient, k_d, it must measure the zinc consumption rate in order to show variables effect on corrosion, where k_d is an indication to reaction rate (corrosion rate). It can be seen from the figure (4) that the zinc consumption rate increases with increasing temperature and flow rate of seawater. It can explain that as follows:

(i) Temperature effect

(1) A temperature increases usually increases the reaction rate which is the corrosion rate and according to the Freundlich equation [Shrier (2), 2000]:

$$Corrosion\ \mathrm{rate} = \mathrm{k\ C_{O_2}^{n}} \qquad \ldots(6)$$

Where k is the rate constant of reaction, C_{O2} is concentration of oxygen and n is order of reaction. The rate constant, k, varying with temperature according to Arrhenius equation [Shrier (2), 2000]:

$$k = k_o e^{-E/RT} \qquad \ldots(7)$$

Where k_o is constant, E is activation energy, R is universal constant and T is temperature. Then from equation (7) indicates that the k is increased with increasing temperature and then the corrosion rate which is lead to increasing the of zinc dissolution.

(2) Increasing seawater temperature leads to decreasing seawater viscosity with a consequent increase in oxygen diffusivity according to Stockes-Einstein equation [Cussler, 1984 and Konsowa and El-Shazly, 2002]:

$$\frac{\mu D}{T} = \mathrm{constant} \qquad \ldots(8)$$

Where μ is seawater viscosity and D is the diffusivity of the dissolved oxygen. As a result of increasing the diffusivity of dissolved oxygen, the rate of mass transfer of dissolved oxygen to the cathodic surface increases according to the following equation [Konsowa and El-Shazly, 2002]:

$$J = k_d C_{O_2} = \frac{D}{\delta_d} C_{O_2} \qquad \ldots(9)$$

With a consequence increase in the rate of zinc dissolution. Where J is mole flux of oxygen.

(3) The decrease in the seawater viscosity with increasing temperature improve the seawater conductivity with a consequent increase in corrosion current and the rate of corrosion.

(4) On the other hand, increase of temperature reduce the solubility of dissolved oxygen with a subsequent decrease in the rate of oxygen diffusion to the cathode surface and the rate of corrosion.

It seems that within the present range of temperature effects 1, 2, and 3 are predominating.

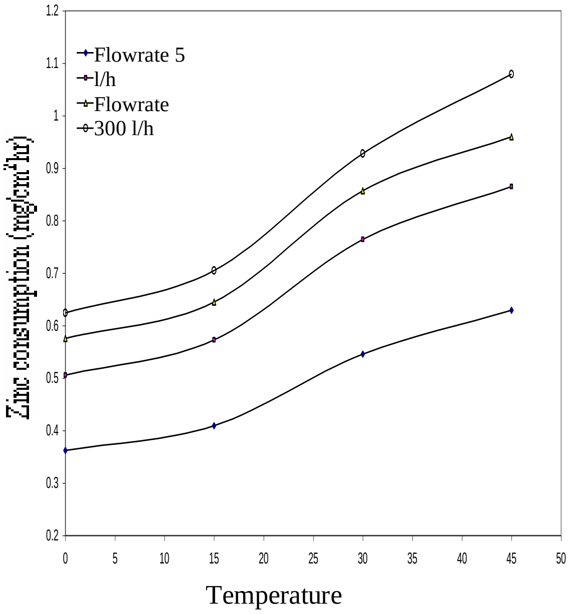

Fig.4. Temperature Effect on Zinc Consumption Rate with Variable Flow Rate.

(ii) Flow rate effect: Increase zinc consumption rate with increasing flow rate is attributed to the decrease in the thickness of hydrodynamic boundary layer and diffusion layer across which dissolved oxygen diffuses to the tube wall of steel with consequent increase in the rate of oxygen diffusion which is given by equation (9). Then the surface film resistance almost vanishes, oxygen depolarization, the products of corrosion and protective film are continuously swept away and continuous corrosion occurs. The flow rate of seawater may also used erosion which combined with electrochemical attack.

Mass transfer coefficient: The mass transfer coefficient can be expressed in terms of the dimensionless Reynolds (Re), Schmidt (Sc) and Sherwood (Sh) numbers. These numbers are defined by [Coulson and Richardson, Vol. 1 & 2, 2002]:

$$\mathrm{Re} = \frac{\rho u d_e}{\mu} \qquad \ldots(10)$$

$$Sc = \frac{\mu}{\rho D} \qquad \ldots(11)$$

$$Sh = \frac{k_d d_e}{D} \qquad \ldots(12)$$

Where ρ is density, u is velocity d_e is equivalent inner tube (based on cross section area of zinc exist in the inner tube], µ is dynamic viscosity D is diffusivity and k_d is mass transfer coefficient. For single phase flow in a straight pipe, the correlation of Berger and Hau (1997) and Anederko et al. (2001) can b used:

$$Sh = 0.0165\,\mathrm{Re}^{0.86}\,Sc^{0.33} \qquad \ldots(13)$$

The physical properties of seawater at pH = 7 are explained in table (3).

Table 3,
Physical Properties of Seawater at pH = 7

Variable	**Temperature °C**			
	0	**15**	**30**	**45**
ρ **(kg/m^3)**	1005.5	1003.9	999.7	995.8
µ (Pa.s)	2×10^{-3}	1.3×10^{-3}	0.91×10^{-3}	0.72×10^{-3}
D **(cm^2/s)**	1.67×10^{-5}	1.8×10^{-5}	1.95×10^{-5}	2.1×10^{-5}

Where ρ is practically measured µ is from Coast (1999) and *D* is from Harvey and Robert, (1988).

To estimate k_d e.g. at 15°C, 300 lit/hr flow rate and d_e = 2.533 cm the velocity u is 16.5 cm/s. Equation (10) gives that Re is 3227, from equation (11) Sc is 719, from equation (13) Sh is 151 and then from equation (12) k_d is 10.73×10^{-6} m/s. Figure (5) shows that the effect of flow rate (i.e. velocity or Re) on k_d with different temperature, where k_d increases with increasing flow rate and temperature according to figure (4).

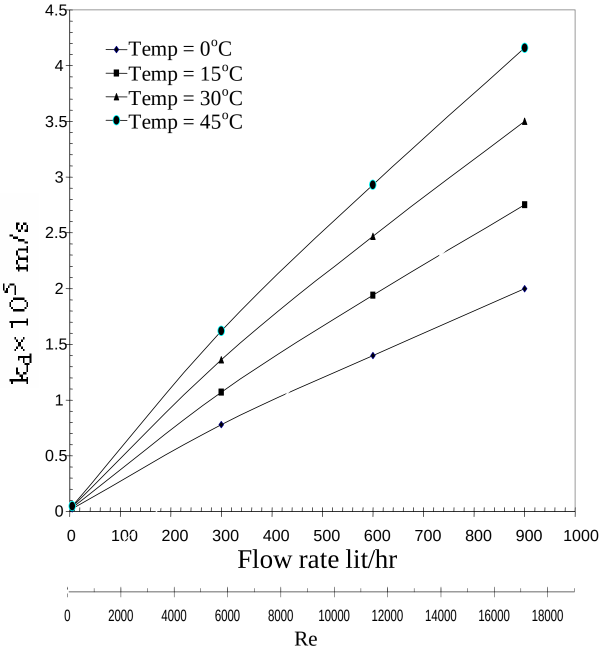

Fig. 5. Effect of Flow Rate (Reynold, s Number) on k_d With Different temperature.

II. Impressed Current System:

Polarization: The characteristic of cathodic polarization curves with variation of temperature and angular velocity have been illustrated in figures (7) to (26). These polarization curves provide information about effects of changes in potential on the corrosion of the cathode as current density (current per unit area). Since the electrolyte is seawater (saltwater), the concentration polarization type is predominant [Ailor, 1971 and Fontana and Green, 1984].

From polarization curves, it can be determined practically the free corrosion potential, E_{corr} and limiting current density, i_L. Where E_{corr} is determined when the potential becomes approximately constant with decreasing current. The limiting current plateau is not well defined, thus the method given by Gabe and Makanjoula (1986) will be adopted to fined i_L values:

$$i_L = \frac{i_1 + i_2}{2} \qquad \ldots(14)$$

Where i_1 and i_2 are the current associated with E_1 and E_2 respectively as shown in figure (6). From figure (7) to (26) one can see that E_{corr} is more negative with increasing temperature and with decreasing velocity. While i_L increases with increasing temperature and velocity. $i_L = i_{corr}$ is indication for corrosion rate, where the high value of i_L means the high corrosion and vise versa. So the interpretation of increasing i_L with increasing temperature and velocity are as mentioned in sacrificial anode system.

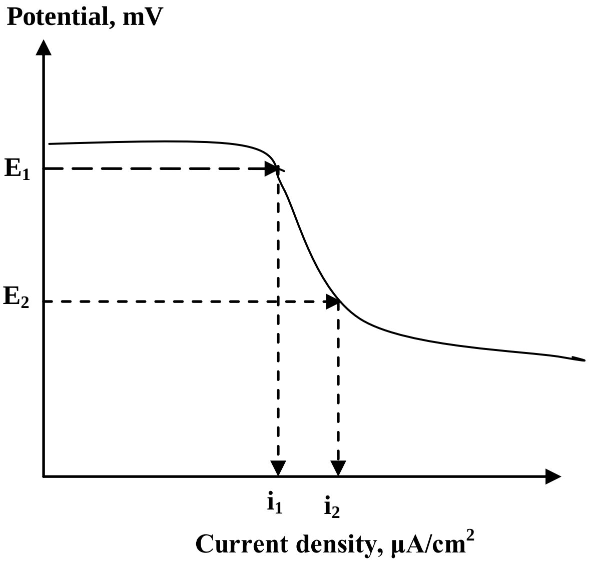

Fig.6. Calculate the Limiting Current Density by Gabe and Makanjoula Method.

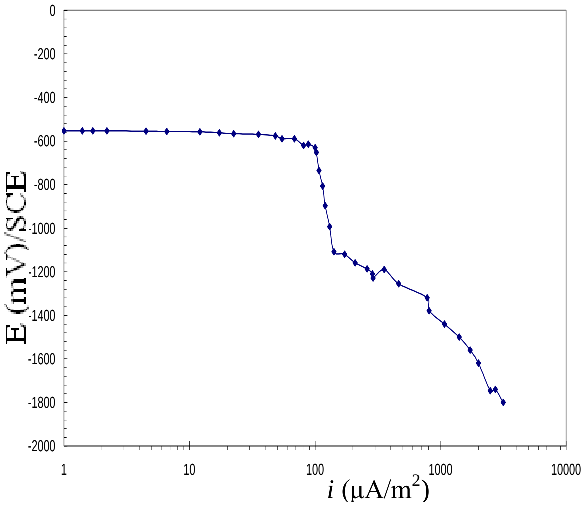

Fig.7. Cathodic Polarization Curve at 0°C and 0 rpm.

For more explicit and simplicity i_L were calculated from figures (7 – 26) using equation (14) and figure (6) and plotting the results in figure (27) with variables.

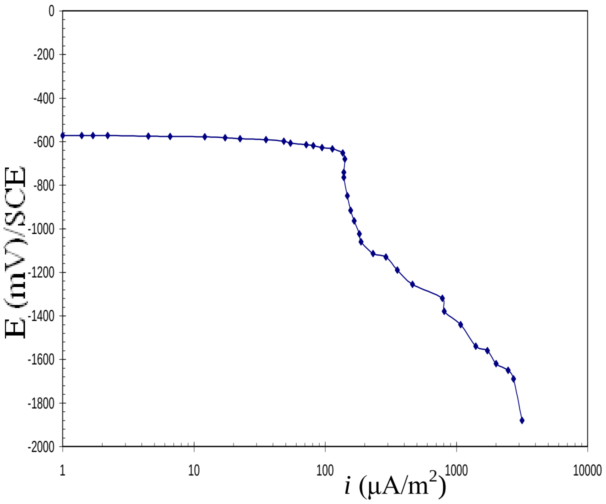

Fig.8. Cathodic Polarization Curve at 15°C and 0 rpm.

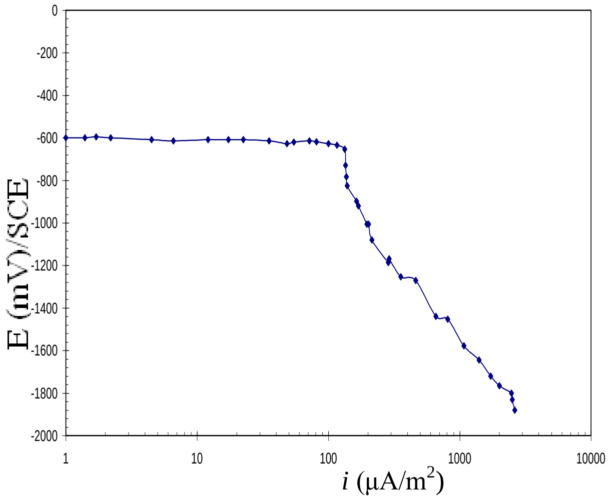

Fig.9. Cathodic Polarization Curve at 30°C and 0 rpm.

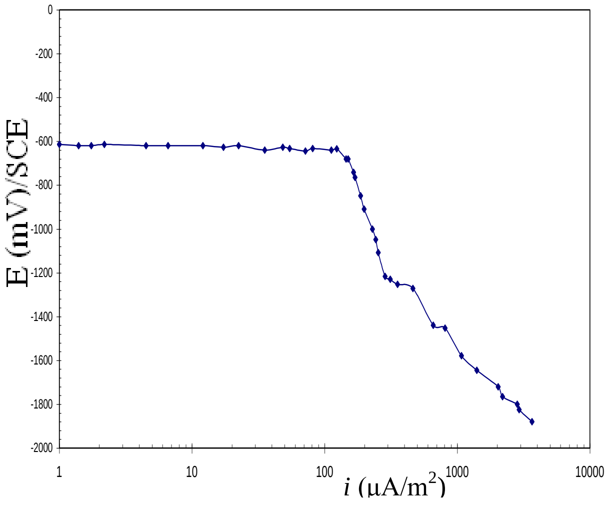

Fig.10. Cathodic Polarization Curve at 45°C and 0 rpm.

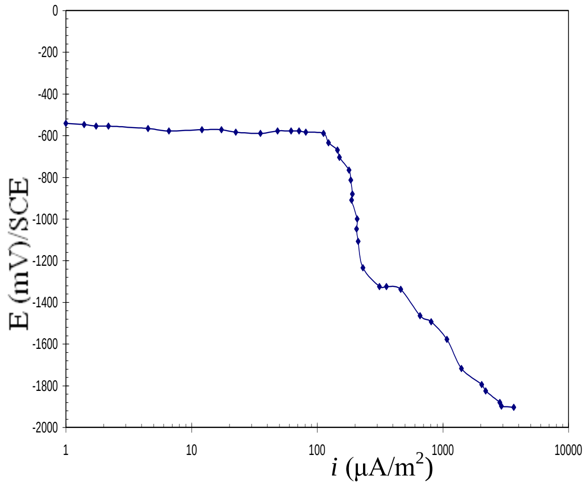

Fig.11. Cathodic polarization curve at 0°C and 100 rpm.

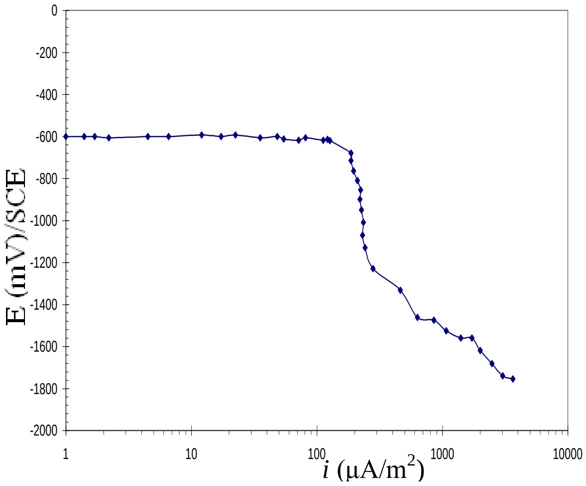

Fig.14. Cathodic Polarization Curve at 45°C and 100 rpm.

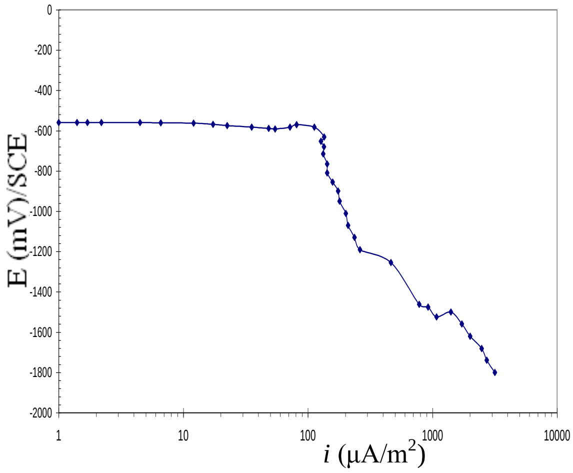

Fig.12. Cathodic Polarization Curve at 15°C and 100 rpm.

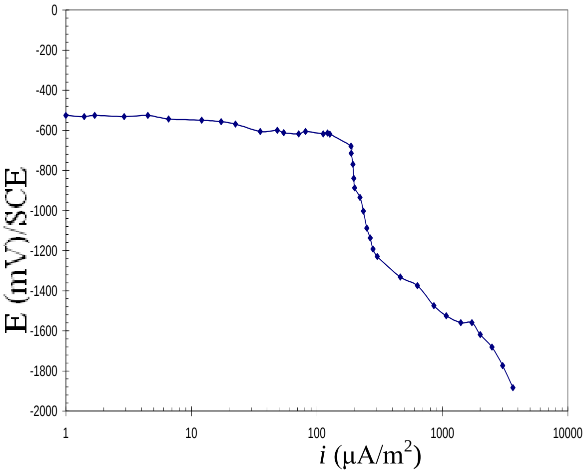

Fig.15. Cathodic Polarization Curve at 0°C and 200 rpm.

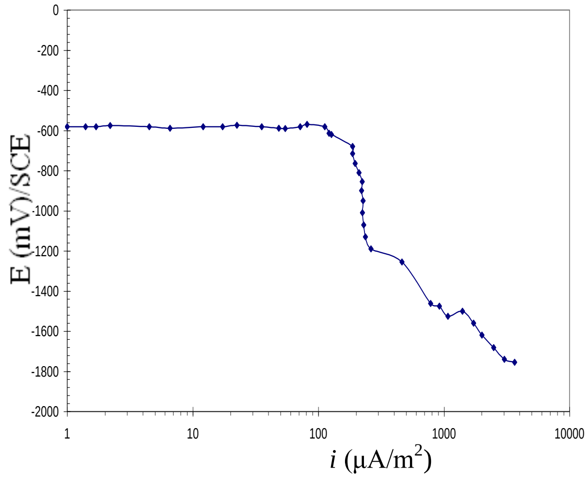

Fig.13. Cathodic Polarization Curve at 30°C and 100 rpm.

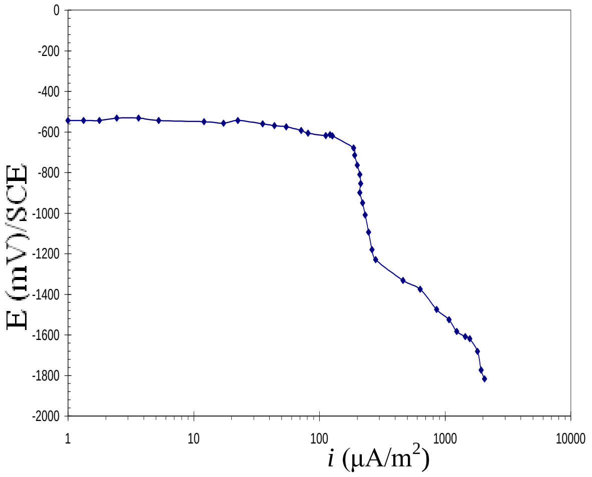

Fig.16. Cathodic Polarization Curve at 15°C and 200 rpm.

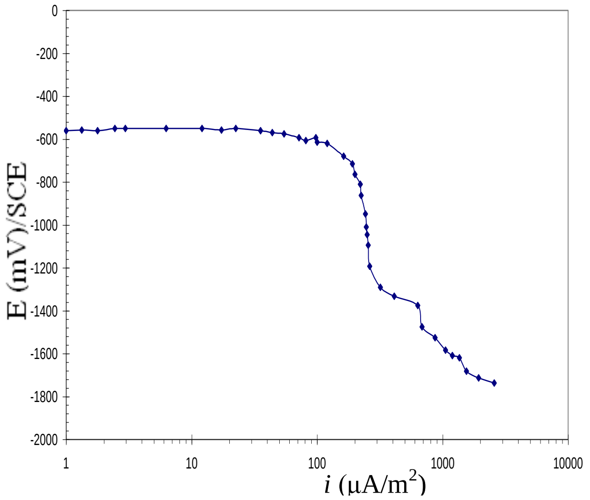

Fig.17. Cathodic Polarization Curve at 30°C and 200 rpm.

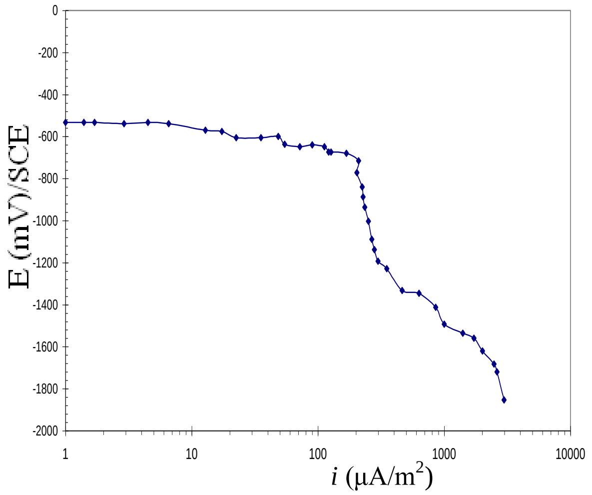

Fig.20. Cathodic polarization curve at 15°C and 300 rpm.

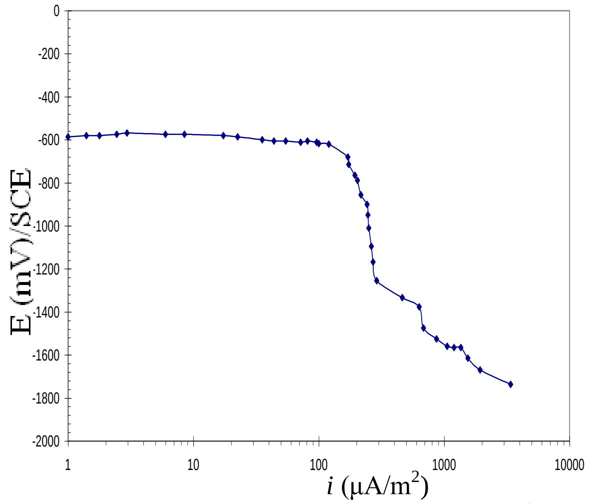

Fig.18. Cathodic Polarization Curve at 45°C and 200 rpm.

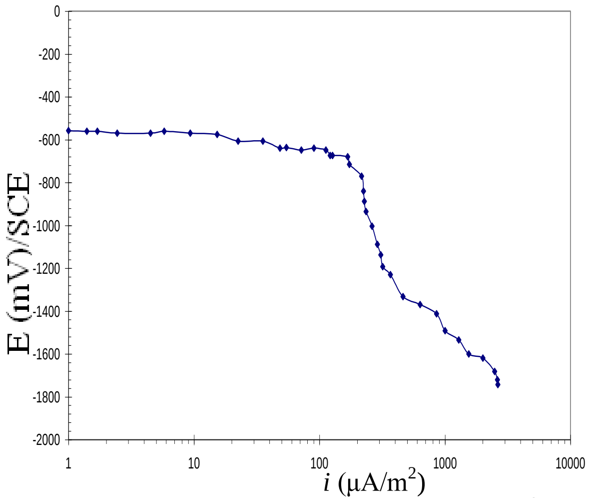

Fig.21. Cathodic Polarization Curve at 30°C and 300 rpm.

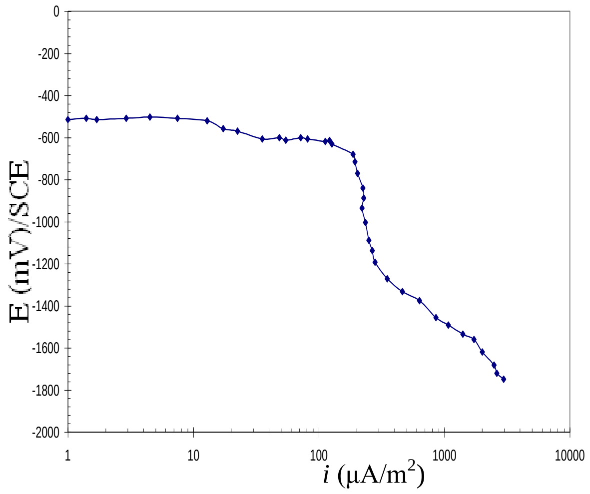

Fig.19. Cathodic Polarization Curve at 0°C and 300 rpm.

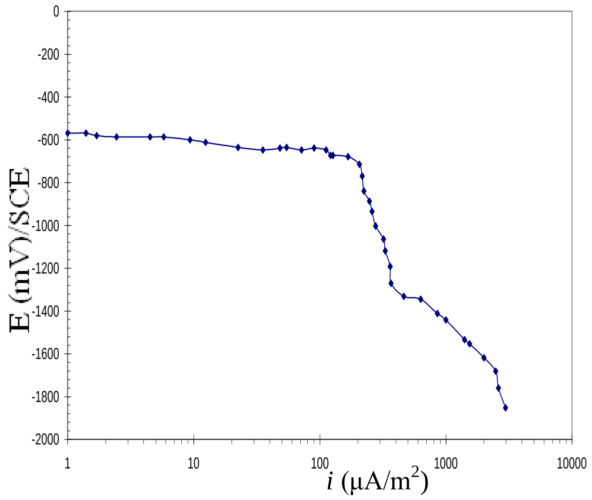

Fig.22. Cathodic Polarization Curve at 45°C and 300 rpm.

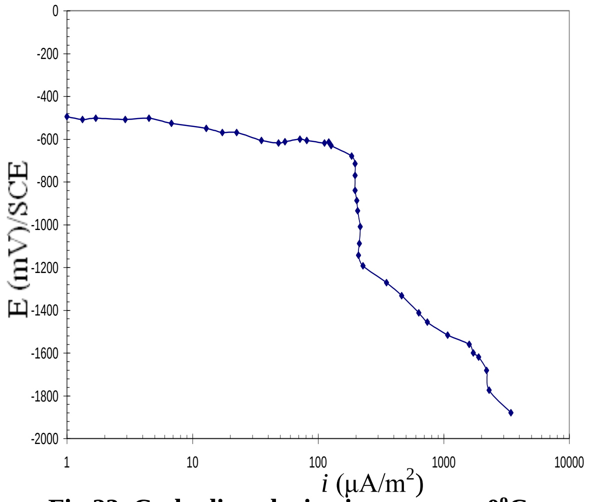

Fig.23. Cathodic polarization curve at 0°C and 400 rpm.

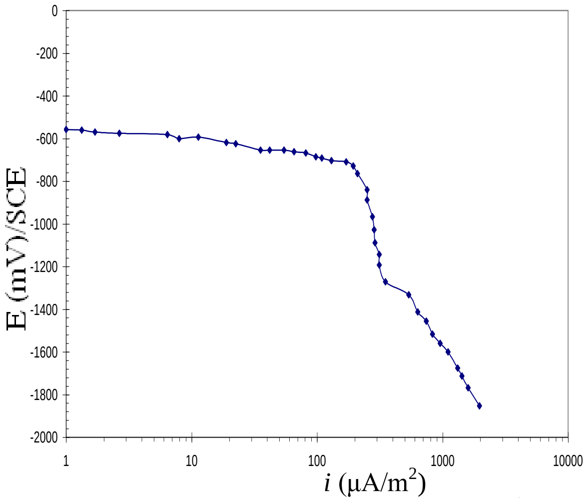

Fig.26. Cathodic polarization curve at 45°C and 400 rpm.

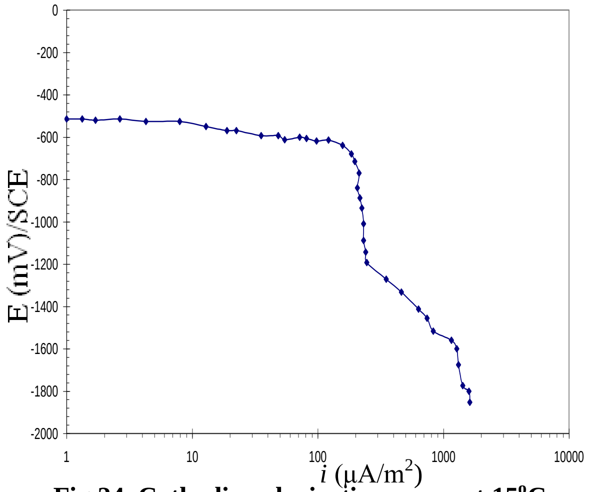

Fig.24. Cathodic polarization curve at 15°C and 400 rpm.

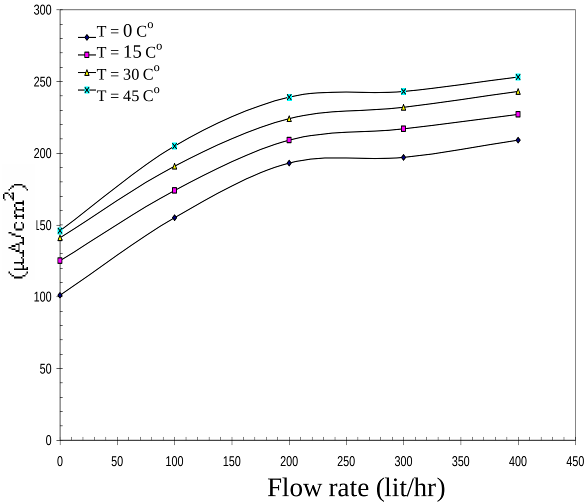

Fig.27. Variation of practical limiting current density with flow rate at different temperature.

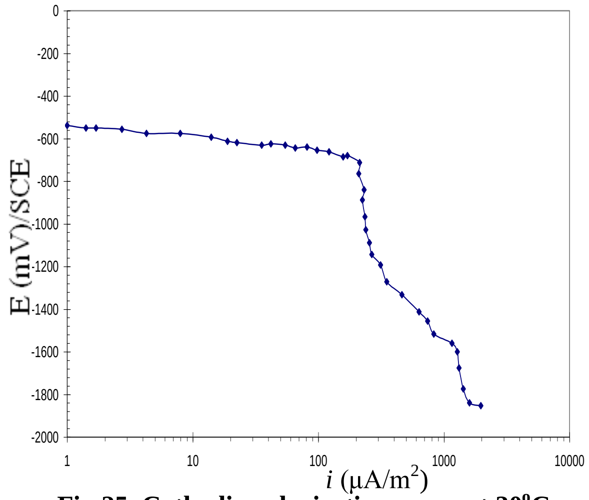

Fig.25. Cathodic polarization curve at 30°C and 400 rpm.

Mass transfer coefficient: when cathodic current is limited by oxygen reduction reaction (as in equation 15) and when oxygen diffusion through a fluid boundary layer limits the supply of oxygen at the specimen surface for a rotating cylinder, equation (16) is applied to calculate mass transfer coefficient, k_d [Shrier (1), 2000 and Silverman, 2004].

$$O_2 + 2H_2O + 4e \rightarrow 4OH^- \qquad \ldots(15)$$

$$k_d = \frac{i_L}{zFC_b} \qquad \ldots(16)$$

It can be seen from equation (16) that that the parameters which can be influence on k_d are i_L and C_b . i_L was estimated from figures (7 – 26) by using the method in figure (6) and equation (14). Figure (28) shows that the variation of k_d with flow rate or Reynolds number at different temperature.

Limiting current density, i_L, can be estimated theoretically from the following equation [Eisenberg et al., 1954 and Harvey and Robert, 1988]:

$$i_L = 0.0791 zFC_b U \,\mathrm{Re}^{-0.3}\, Sc^{-0.644} \qquad \ldots(17)$$

So from equations (16) and (17) the k_d is estimated as:

$$k_d = 0.0791\, U\, \mathrm{Re}^{-0..3}\, Sc^{-0.664} \qquad \ldots(18)$$

Where U is the tangential velocity of specimen surface ($\pi \times d \times$rpm/60), d is the diameter of specimen cylinder (2.33 cm), z is the number of electrons in reduction reaction of oxygen (equation (15)) which is equal to 4 eq/mol, C_b is the concentration of oxygen in bulk [Shrier,1, 2000] and F is Faraday's number (96494 c/eq). Reynolds and Schmidt numbers are estimted as in equations (10) and (11), respectively. Figure (29) shows mass transfer coefficient, k_d, which was estimated theoretically versus Reynolds number at different temperature. It can be noted that k_d increases with *Re* (or rotation velocity, ω) and with increasing T, that's mean increasing corrosion rate with increasing ω and T.

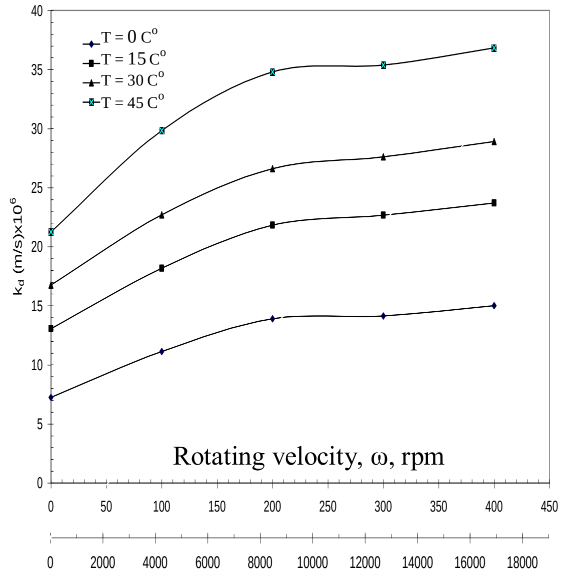

Fig.28. variation of mass transfer coefficient practically with Re at different Temperature.

It can be seen that there is a difference between figures (28) and (29) because k_d in figure (29) was estimated from equation (18) where the velocity is affected mainly on k_d where if the velocity is zero the k_d will be zero while practically k_d has some value at zero velocity. So the range of rotation velocity in figure (29) was taken from 50 to 400 rpm to avoid zero value of k_d.

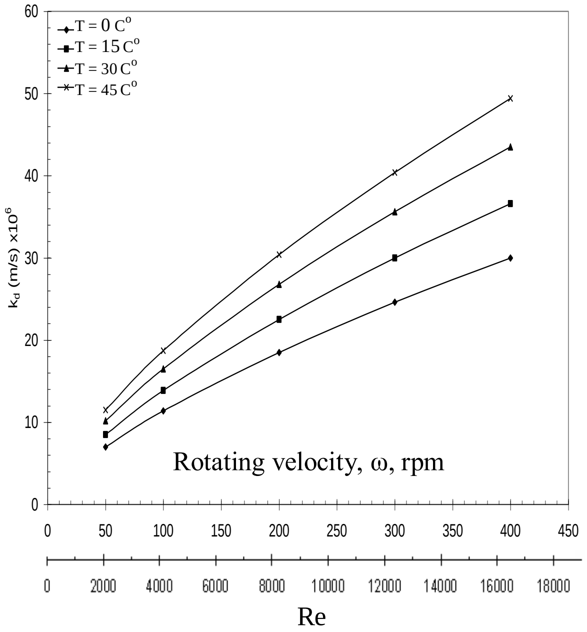

Fig.29. variation of mass transfer coefficient theoretically with Re at different Temperature.

4. Conclusions

1. In the sacrificial anode cathodic protection (SACP) method the mass transfer coefficient k_d increases with increasing volumetric flow rate or Reynolds number and with increasing temperature that's mean the corrosion rate increases with two variables above.
2. In the impressed current cathodic protection (ICCP) method, kd increases with increasing rotation velocity or Reynolds number and with temperature.
3. There is some a difference between the practical results and theoretical results of the k_d in the ICCP.

5. References

[1] Ailor, W. H. (1971), "Handbook on corrosion testing and evaluation", John Wiley and Sons Inc.

[2] Anderko, A., McKenzie, P. and Young, R. D. (2001), "Computation of rates of general corrosion using electrochemical and thermodynamic modes corrosion".

[3] Berger, F. P., Hau, K-F. F. L. (1977), Int. J. Heat Mass Transfer, 20, pp 1185-1194.

[4] Champion, F. A. (1964), "Corrosion testing procedures", 2nd edition.

[5] Coast Guard U.S. (1999), Chemical Hazardous Response Information System (CHRIS), selected properties of fresh water, seawater, ice and air.

[6] Cornet I. and Kappesser, R. (1969), "Cathodic protection of a rotating cylinder", Trans.

[7] Instn. Chem. Engrs., 47.

[8] Cottis, R. A. (2002), "Electrochemical kinetics and thermodynamics".

[9] Coulson, J. M. and Richardson, J. F. "Chemical engineering", Vol. 1 (1999) and vol. 2 (2002).

[10] Cussler, E. L. (1984), "Mass transfer in fluid systems", Cambridge University press, Cambridge, UK.

[11] Eisenberg, M., Toblas, C. W. and Wilke, R. C. (1954), J. Electrochemical Society, 101 (6), pp 306-319.

[12] Fontana, M. G. and Greene, N. D. (1984), "Corrosion engineering", 2nd edition, McGraw-Hill.

[13] Gabe, D. R. and Makanjoula, P. A. (1986), EFCF Publication Series No. 15, "electrochemical engineering", AIChE Symposium Series, (98), p. 309.

[14] Hanson, H. R. (2000), "Offshore cathodic protection guidelines: relevance of short term laboratory testing". (Internet site: www.corrosionsource.com).

[15] Harvey, P. H. and Robert J. G. (1988), paper no. 38, Corrosion 88, March 21-25.

[16] Konsowa, A. H. and El-Shazly, A. A. (2002), Elsevier, Desalination, 153, pp 223-226.

[17] Roberge, R. P. (1999), "Handbook of corrosion engineering".

[18] Roberge, R. P. (2004), "Electrochemical kinetics principles nearest diffusion layer ". (internet site: www.corrosiondoctor.org)

[19] Scully, J. C. (1975), "The fundamental of corrosion", 2nd edition.

[20] Shrier (1), L. L. (1976), "Corrosion 1, metal/environment reactions", Newnes-Butterworth.

[21] Shrier (1), L. L. (2000), "Corrosion 1, metal/environment reactions", Newnes-Butterworth.

[22] Shrier (2), L. L. (2000), "Corrosion 2, corrosion control", 3rd edition, Newnes-Butterworth.

[23] Trethewey, K. R. and Chamberlain, J. (1996), "Corrosion for scientist and engineering", 2nd edition.

[24] Uhlig, H. H. (1971), "Corrosion and corrosion control, an introduction to corrosion science and engineering", John-Wiley and Sons.

معامل انتقال المادة خلال الحماية الكاثودية لحديد واطئ الكاربون في مياه البحر

د. خالد وليد حميد* ، **أنيس عبد الله كاظم****، **أميل محمد رحمن***

كلية الهندسة الخوارزمي / جامعة بغداد / قسم الهندسة الكيميائية الأحيائية

*** كلية الهندسة / جامعة ديالى*

الخلاصة

الهدف من البحث هو حساب معامل انتقال المادة، k_d ، خلال الحماية الكاثودية لحديد واطئ الكاربون في مياه البحر المتعادل (3.5% $NaCl$ وزن\حجم في الماء المقطر و دالة حامضية = 7). تم استخدام طريقتين من الحماية الكاثودية:

الاولى: الحماية الكاثودية بطريقة أنود التضحية لأنبوب الحديد حاملاً مياه البحر بأستخدام قطب الخارصين كأنود تضحية عند المتغيرات الاتية: درجة الحرارة بمدى (0 – 45 ْم) ومعدل جريان حجمي بمدى (5 – 900 لتر\ساعة). لقد وجد أن k_d يزداد بزيادة درجة الحرارة وزيادة معدل الجريان الحجمي او رقم رينولد ، حيث تراوحت قيمة k_d ($0.24\times10^{-6} – 41.6\times10^{-6}$ m/s).

الثانية: الحماية الكاثودية بطريقة التيارالمسلط لأسطوانة حديدية مدورة عمودياً في مياه البحر المتعادل عند المتغيرات الاتية: درجة الحرارة بمدى (0 – 45 ْم) وسرعة تدوير بمدى (0 – 400 دورة\دقيقة). لقد وجد أن k_d يزداد بزيادة درجة الحرارة وزيادة سرعة تدوير الاسطوانة او رقم رينولد، حيث تراوحت قيمة k_d ($7.25\times10^{-6} – 36.82\times10^{-6}$ m/s).
